

## Self-Assembled Nanocages for Hydrophilic Guest Molecules

Marie-Christine Jones,<sup>†</sup> Pankaj Tewari,<sup>†</sup> Claudia Blei,<sup>†</sup> Kelly Hales,<sup>‡</sup>  
Darrin J. Pochan,<sup>‡</sup> and Jean-Christophe Leroux<sup>\*,†,§</sup>

Contribution from the Canada Research Chair in Drug Delivery, Faculty of Pharmacy, Université de Montréal, P.O. Box 6128, Downtown Station, H3C 3J7 Montreal, Quebec, Canada, and Materials Science and Engineering and Delaware Biotechnology Institute, University of Delaware, Newark, Delaware 19176

Received July 28, 2006; E-mail: jean-christophe.leroux@umontreal.ca

**Abstract:** Reverse polymeric micelles are obtained following the association of polymeric amphiphiles in apolar media. To this date, reports of pharmaceutical applications for such micelles have been scarce, mainly because these systems have been studied in solvents that are not suitable for medical use. Here, alkylated star-shaped poly(glycerol methacrylate) polymers have been proposed in the design of oil-soluble reverse polymeric micelles. Micellar behavior was studied in various apolar solvents, including ethyl oleate, a pharmaceutically acceptable vehicle. The polymers were shown to assemble into spherical nanostructures (<40 nm) as determined by cryogenic transmission electron microscopy and atomic force microscopy studies. Interestingly, the reverse micelles were able to encapsulate various peptides/proteins (vasopressin, myoglobin, and albumin) in substantial amounts and facilitate their solubilization in oil. The nature of both the polymer used in micelle formation and the guest molecules was found to influence the ability of the micelle to interact with hydrophilic compounds.

## 1. Introduction

The ability of micellar aggregates to act as solubility enhancers stems from the dichotomy of their architecture. Indeed, the segregation of the lyophobic segment of an amphiphilic compound in the micelle core allows for the creation of a favorable micro-environment for molecules with limited affinity for the dispersing phase. Theoretically, reverse micelles should be obtained from any amphiphilic molecules placed in an organic, nonpolar solvent. However, for most low-molecular-weight surfactants, the presence of water or another polar solvent appears to be necessary for micelle formation.<sup>1–5</sup> Consequently, these systems consist of a polar phase stabilized by a molecular surfactant layer in an arrangement reminiscent of a water-in-oil microemulsion. Nevertheless, several reports have emerged on potential applications for these reverse micelles, including their use as nanoreactors,<sup>6</sup> for protein encapsulation,<sup>7</sup> for extraction of water-soluble biomolecules,<sup>8</sup> or in protein conformational studies.<sup>9</sup> The assembly of surfactant-based reverse

micelles has mainly been studied in organic solvents such as saturated hydrocarbons, and few examples of their use in pharmaceutically relevant vehicles have been reported.<sup>10,11</sup>

Hydrophobically modified dendrimers and hyperbranched polymers were recently proposed for the design of unimolecular reverse polymeric micelles. Both types of polymers are characterized by relatively compact structures with high densities of surface functionalities.<sup>12</sup> Compared to dendrimers, hyperbranched polymers present the added benefit of being easier to prepare.<sup>13</sup> Reverse unimolecular micelles are typically generated by the partial modification of surface hydroxyl or amine functions with fatty acid derivatives. Such polymeric structures have been shown to promote the extraction and solubilization of various hydrophilic model compounds in nonpolar organic solvents. For instance, Cooper et al.<sup>14</sup> highlighted the use of reverse polymeric micelles (RPMs) for improving the solubility of a water-soluble dye in supercritical carbon dioxide. Later, reverse micelles obtained from hyperbranched poly(glycerol)s<sup>15</sup> or poly(ethylenimine)s<sup>16</sup> were shown to extract the hydrophilic dye Congo red from water into chloroform. The potential

<sup>†</sup> Université de Montréal.<sup>‡</sup> University of Delaware.<sup>§</sup> Canada Research Chair in Drug Delivery.

- (1) Price, K. E.; McQuade, D. T. *Chem. Commun.* **2005**, 1714–1716.
- (2) Pileni, M. P. *Nat. Mater.* **2003**, *2*, 145–150.
- (3) Carvalho, C. M. L.; Cabral, J. M. S. *Biochimie* **2000**, *82*, 1063–1085.
- (4) Riter, R. E.; Kimmel, J. R.; Undikis, E. P.; Levinger, N. E. *J. Phys. Chem. B* **1997**, *101*, 8292–8297.
- (5) Khougaz, K.; Gao, Z. S.; Eisenberg, A. *Langmuir* **1997**, *13*, 623–631.
- (6) Mecking, S.; Thomann, R.; Frey, H.; Sunder, A. *Macromolecules* **2000**, *33*, 3958–3960.
- (7) Luisi, P. L.; Giomini, M.; Pileni, M. P.; Robinson, B. H. *Biochim. Biophys. Acta* **1988**, *947*, 209–246.
- (8) Fadnavis, N. W.; Satyavathi, B.; Deshpande, A. A. *Biotechnol. Prog.* **1997**, *13*, 503–505.
- (9) Van Horn, W. D.; Simorellis, A. K.; Flynn, P. F. *J. Am. Chem. Soc.* **2005**, *127*, 13553–13560.

- (10) Ichikawa, S.; Sugiura, S.; Nakajima, M.; Sano, Y.; Seki, M.; Furusaki, S. *Biochem. Eng. J* **2000**, *6*, 193–199.
- (11) New, R. R. C.; Kirby, C. J. *Adv. Drug Delivery Rev.* **1997**, *25*, 59–69.
- (12) Stevelmans, S.; Hest, J. C. M.; Jansen, J. F. G. A.; Van Boxtel, D. A. F. G.; Da Brabander-van den Berg, E. M. M.; Meijer, E. W. *J. Am. Chem. Soc.* **1996**, *118*, 7398–7399.
- (13) Sunder, A.; Bauer, T.; Mülhaupt, R.; Frey, H. *Macromolecules* **2000**, *33*, 1330–1337.
- (14) Cooper, A. I.; Londono, J. D.; Wignall, G.; McClain, J. B.; Samulski, E. T.; Lin, J. S.; Dobrynin, A.; Rubinstein, M.; Burke, A. L. C.; Frechet, J. M. J.; Desimone, J. M. *Nature (London)* **1997**, *389*, 368–371.
- (15) Sunder, A.; Krämer, M.; Hanselmann, R.; Mülhaupt, R.; Frey, H. *Angew. Chem., Int. Ed.* **1999**, *38*, 3552–3555.
- (16) Chen, Y.; Shen, Z.; Frey, H.; Perez-Prieto, J.; Stiriba, S.-E. *Chem. Commun.* **2005**, 755–757.

of RPMs as drug delivery systems was demonstrated using hydrophobically modified poly(amidoamine) dendrimers for the oral administration of 5-fluorouracil, an anticancer drug.<sup>17</sup> While they are good at solubilizing monomolecular entities, unimolecular reverse micelles present limited core space, which may not be suitable for the incorporation of larger guests such as proteins. In the present study, it was hypothesized that the encapsulation of more complex structures could be better achieved using multimolecular reverse micelles. Accordingly, RPMs were prepared from amphiphilic star-shaped poly-(alcohol)s, and their behavior was studied in various organic phases. More specifically, RPMs were evaluated for their ability to enhance the solubility of peptides/proteins in ethyl oleate, a solvent accepted for pharmaceutical use. It is expected that the formulation of these compounds in an oleaginous environment will improve their stability against enzymatic degradation and promote their absorption through biological barriers such as the intestinal membrane.<sup>11</sup> If administered subcutaneously, the RPM formulation could also serve as a reservoir for the sustained release of peptidic drugs. Here, four-arm poly(glycerol methacrylate)s were employed as scaffolds in the elaboration of RPMs. The hydrophobicity of the micellar shell was tailored using fatty acid derivatives of varying length. The micelles were characterized with regard to their assembly in tetrahydrofuran (THF) and ethyl oleate, and their ability to interact with hydrophilic macromolecules was studied using three peptidic molecules, namely vasopressin, myoglobin, and albumin.

## 2. Experimental Section

**2.1. Materials.** Glycidyl methacrylate was obtained from Poly-science (Warrington, PA). Other reagents employed in polymer synthesis were purchased from Aldrich (Oakville, ON, Canada) and used without further purification. THF was dried over sodium using benzophenone as a dryness indicator. Myoglobin and fluorescein–isothiocyanate conjugate albumin (FITC-albumin) were obtained from Sigma (Oakville, ON, Canada).

**2.2. Methods.** **2.2.1. Synthesis of Star-Shaped Poly(glycidyl methacrylate) (PGMA).** Atom-transfer radical polymerization (ATRP) was carried out in THF using copper bromide (Cu<sup>I</sup>Br) as a catalyst and 1,2-bipyridyl as a ligand. ATRP initiator, tetrakis(2-bromoiso-butryl) pentaerythritol<sup>18</sup> (1 equiv) was added to Cu<sup>I</sup>Br (1 equiv), 1,2-bipyridyl (1 equiv), and glycidyl methacrylate (106 equiv) in THF ([monomer] = 0.3 M). The mixture was degassed under argon for 15 min at room temperature and then heated to 90 °C. The reaction was left to proceed for 24 h. The mixture was then poured into THF containing ethanol (95:5) and passed through a silica gel column to remove the copper. THF was used as eluent. The solvent was evaporated under reduced pressure, and the crude polymer extract was precipitated twice in diethyl ether. The polymer was further purified by Soxhlet extraction in diethyl ether. A mean degree of polymerization of 26 units per initiator arm was targeted for a total molecular weight (MW) of 15 000. Number- ( $M_n$ ) and weight-average ( $M_w$ ) MWs were determined using a Waters 1525 size exclusion chromatography (SEC) system equipped with a 2410 refractometer (Waters, Milford, MA) and a low-angle laser light scattering detector (PD2000DLS, Precision Detectors, Bellingham, MA). Analyses were performed in *N,N*-dimethylformamide with 10 mM LiBr at a flow rate of 1 mL/min using a set of three Styragel HT2, HT3, and HT4 columns (Waters), maintained at 45 °C. <sup>1</sup>H NMR spectra were recorded on a Bruker

ARX400 spectrometer in deuterated chloroform (CDCl<sub>3</sub>). <sup>1</sup>H NMR ( $\delta$ , ppm, CDCl<sub>3</sub>): 4.31 (m, 112H); 4.1 (m, 7.99H); 3.8 (m, 113H); 3.22 (m, 114H); 2.84 (m, 115H); 2.63 (m, 116H); 1.8–2.2 (m, 208H); 0.9–1.1 (m, 349H).

**2.2.2. Synthesis of Star-Shaped Poly(glycerol methacrylate) (PG<sub>OH</sub>MA).** PG<sub>OH</sub>MA was obtained following the hydrolysis of the epoxy ring of PGMA. In a typical procedure, PGMA (6 g) was dissolved in 1-methyl-2-pyrrolidinone (NMP, 75 mL) under gentle stirring. After complete dissolution of the polymer, 15 mL of water was added dropwise, and the mixture was left to react at 140 °C for 24 h. The hydrolyzed polymer was dialyzed (Spectra/Por no. 1, MW cutoff 2000, Spectrum Laboratories, Rancho Dominguez, CA) against water for 48 h and then freeze-dried. <sup>1</sup>H NMR spectra were recorded on a Bruker ARX400 spectrometer in deuterated dimethyl sulfoxide (DMSO-*d*<sub>6</sub>). <sup>1</sup>H NMR ( $\delta$ , ppm, DMSO-*d*<sub>6</sub>): 4.7–4.9 (m, 2H); 3.7–3.9 (m, 3H); 3.3 (m, 48H); 1.82 (m, 1.4H); 0.4–1.2 (m, 3H).

**2.2.3. Synthesis of Hydrophobically Modified Star-Shaped (PG<sub>OH</sub>MA-CX).** PG<sub>OH</sub>MA (228 equiv of hydroxyl group) was dried by azeotropic distillation and solubilized in pyridine (0.8 M) in the presence of catalytic amounts of 1-methylimidazole. Acyl chloride derivatives (137 equiv) were dissolved in toluene and slowly added to the reaction mixture under anhydrous and inert conditions. The reaction was left to proceed overnight under reflux. K<sub>2</sub>CO<sub>3</sub> (5 g) was added following completion of the reaction. Excess pyridine was removed under reduced pressure. The mixture was then transferred to a separation funnel with 200 mL of chloroform, and pyridine residues were extracted successively with HCl (0.1 M) and brine. The organic extracts were dried over MgSO<sub>4</sub>, filtered, and dialyzed against chloroform for 24 h (Spectra/Por Biotech regenerated cellulose, MW cutoff 6000–8000, Spectrum Laboratories). The solvent was removed under reduced pressure to yield the alkylated polymer as off-white waxy flakes. All star-shaped amphiphilic polymers are referred to as PG<sub>OH</sub>MA-CX, where X stands for the total number of carbon atoms present on the fatty acid chain.

**2.2.4. Determination of the Degree of Alkylation.** The degree of alkylation (DA) was determined from the <sup>1</sup>H NMR spectra of PG<sub>OH</sub>MA-CXs using eq 1,

$$DA = \frac{I(5DP + 8)}{20DP(n - 4) + 10DP} \times 100 \quad (1)$$

where *I* is the intensity of the peak at  $\delta = 1.2$ – $1.3$  ppm, DP is the degree of polymerization calculated from the <sup>1</sup>H NMR of PGMA, and *n* is the number of carbon atoms in the alkyl chain.

**2.2.5. Particle Size Analysis.** Dynamic light scattering experiments were performed in THF and ethyl oleate (Crodamol EO, Croda Canada Ltd., Vaughan, ON, Canada) at 25 °C and at an angle of 173° using a Malvern Zetasizer ZS instrument (Malvern, Worcestershire, UK). The polymer concentration was kept constant at 1 g·L<sup>-1</sup>, and peptide concentration was kept at 1 wt % where applicable. All polymer solutions were filtered twice prior to analysis using 0.22- $\mu$ m hydrophilic propylene (GHP) filters. Viscosity values of 0.455 and 9.29 cP (determined experimentally) were employed for THF and ethyl oleate, respectively. The theoretical diameter of a fully extended PG<sub>OH</sub>MA backbone was calculated on the basis of the length of a saturated carbon–carbon bond length (1.54 Å) and the degree of polymerization obtained by <sup>1</sup>H NMR.

**2.2.6. Atomic Force Microscopy (AFM) Imaging.** Forty microliters of a solution of the polymer in THF (0.1 mg·mL<sup>-1</sup>) was deposited on a mica sheet (1 × 1 cm<sup>2</sup>) and centrifuged at 2000 rpm during 2 min using a spin coater (model WS400-A6NPP-lite, Laurell Technologies, North Wales, PA). The samples were vacuum-dried for 24 h before AFM imaging. AFM images were recorded in tapping mode on a Nanoscope IIIa Dimension 3100 instrument (Digital Instruments, Santa Barbara, CA).

**2.2.7. Cryogenic Transmission Electron Microscopy (cryo-TEM) Analysis.** For cryo-TEM imaging, a thin film of polymer solution in

(17) Tripathi, P.; Khopade, A. J.; Nagaich, S.; Shrivastava, S.; Jain, S.; Jain, N. *Pharmazie* **2002**, *57*, 261–264.

(18) Jones, M.-C.; Ranger, M.; Leroux, J.-C. *Bioconjugate Chem.* **2003**, *14*, 774–781.

ethyl oleate was transferred to carbon-coated copper grids. The grids were plunged into liquid ethane at  $-170\text{ }^{\circ}\text{C}$  using a FEI Vitrobot (FEI Co., Hillsboro, OR), an automated cryo preparation system. The vitrified samples were transferred to a Gatan 626 cryoholder and cryotransfer stage. During observation of the vitrified samples, the cryoholder temperature was maintained at  $-170\text{ }^{\circ}\text{C}$ . Images of the vitrified samples were taken in bright-field mode with a Tecnai G2 12 transmission electron microscope (FEI Co.) at 120 kV accelerating voltage.

**2.2.8. Determination of the Partition Coefficient of Vasopressin between Ethyl Oleate and Water.** Hydrophobically modified  $\text{PG}_{\text{OH}}\text{MA}$ s were dissolved in dichloromethane (DCM) (2.5 or 5  $\text{mg}\cdot\text{mL}^{-1}$ ; 1 mL of DCM) and mixed with increasing volumes of an ethanolic solution of vasopressin (Peptide International, Louisville, KY) spiked with  $^3\text{H}$ -vasopressin (Perkin-Elmer, Boston, MA). Ethyl oleate (500  $\mu\text{L}$ ) was added to the mixture. The volatile organic solvents were removed under vacuum. At that point, 500  $\mu\text{L}$  of water was added. The two phases were gently mixed together for 24 h. Following complete phase separation, 100- $\mu\text{L}$  aliquots of both the aqueous and organic layers were assayed for radioactivity on a LKB-Wallac 1217 Rackbeta liquid scintillation counter (Perkin-Elmer) using Ultima Gold scintillation cocktail (Perkin-Elmer). Controls without polymer were also prepared.

**2.2.9. Extraction of Myoglobin and Albumin.** Small volumes of a concentrated solution (100  $\text{g}\cdot\text{L}^{-1}$ ) of the polymer in ethyl oleate were mixed with predetermined volumes of a solution of myoglobin (1  $\text{g}\cdot\text{L}^{-1}$ ) or FITC-albumin (1  $\text{g}\cdot\text{L}^{-1}$ ) in phosphate-buffered saline (PBS, 75 mM NaCl, 53 mM  $\text{Na}_2\text{HPO}_4$ , 17 mM  $\text{NaH}_2\text{PO}_4$ , pH 7.4) and left to stand at room temperature. In the event of gel formation, the mixture was heated at  $37\text{ }^{\circ}\text{C}$  in order to destroy the organogel. Both phases were completed to their final volume (polymer concentration 5  $\text{g}\cdot\text{L}^{-1}$ ) and gently stirred for 24 h. Sample were centrifuged at 5000g (Hermle Z252M microcentrifuge, Mandel Scientific, Guelph, ON, Canada) for 3 min to induce phase separation. The protein content was assayed in the aqueous layer by spectrophotometry for both myoglobin ( $\lambda_{\text{max}} = 410\text{ nm}$ ) and FITC-albumin ( $\lambda_{\text{max}} = 494\text{ nm}$ ) on a BioTek PowerWave X (Winooski, VT) plate reader. Controls without polymer were also prepared.

**2.2.10 Analysis of Extraction Data.** The percentage of peptide/protein retained in ethyl oleate was calculated from eq 2,

$$\% \text{ retained in ethyl oleate} = \frac{C_{\text{EO}}}{C_{\text{EO}} + C_{\text{W}}} \times 100 \quad (2)$$

where  $C_{\text{EO}}$  and  $C_{\text{W}}$  are the final peptide/protein concentrations in the oil and aqueous phase in the presence of RPMs, respectively. Results are presented as the mean  $\pm$  SEM of at least three independent experiments.

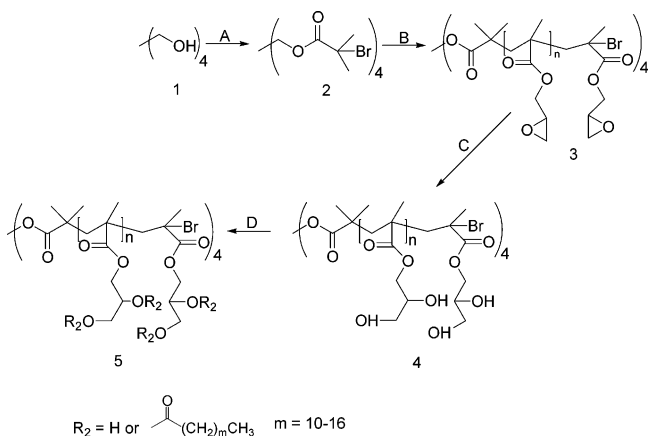
The apparent partition coefficient ( $K_{\text{app}}$ ) of peptide/protein between the organic and aqueous phases was calculated using eq 3,

$$K_{\text{app}} = \frac{C_{\text{EO}}}{C_{\text{W}}} \quad (3)$$

### 3. Results and Discussion

**3.1. Polymer Synthesis.** Amphiphilic  $\text{PG}_{\text{OH}}\text{MA-CX}$ s were selected as building blocks to form multimolecular RPMs. The rationale was that a star-shaped conformation would allow sufficient mobility within the polymer structure to permit hydrogen bond formation between neighboring polymers<sup>19,20</sup> and subsequent aggregation. Star-shaped PGMA was synthesized

**Scheme 1.** Synthesis of Alkylated Star-Shaped  $\text{PG}_{\text{OH}}\text{MA}$ <sup>a</sup>



<sup>a</sup> Reaction conditions: (A) Pentaerythritol (**1**) was esterified with 2-bromoisobutyryl bromide in the presence of triethylamine in THF at room temperature. (B) The ATRP initiator (**2**) was reacted with glycidyl methacrylate (GMA) in THF in the presence of  $\text{Cu}^{\text{I}}\text{Br}/1,2\text{-bipyridyl}$ . (C) PGMA (**3**) was hydrolyzed in a mixture of NMP/ $\text{H}_2\text{O}$  (5:1) to yield star-shaped  $\text{PG}_{\text{OH}}\text{MA}$ . (D)  $\text{PG}_{\text{OH}}\text{MA}$  (**4**) was partially esterified using alkanoyl chlorides in pyridine in the presence of 1-methylimidazole at  $140\text{ }^{\circ}\text{C}$ .

by ATRP from a four-arm multifunctional initiator, namely tetrakis(2-bromoisobutyryl) pentaerythritolate<sup>18</sup> (Scheme 1).

The reaction proceeded smoothly, with over 85% of the monomer converted in 24 h. Polymerization was initiated equally at all sites, and the star conformation was retained as evidenced by AFM (see Supporting Information). The molecular weight of the polymer was evaluated by SEC and  $^1\text{H}$  NMR (Table 1). The results correlated well with the expected value.

The pendant epoxides were hydrolyzed in a mixture of NMP and water to yield the star-shaped  $\text{PG}_{\text{OH}}\text{MA}$  core. The hydrophilic  $\text{PG}_{\text{OH}}\text{MA}$  core was rendered more hydrophobic through chemical modification of the pendant  $-\text{OH}$  functionalities (Scheme 1). The latter were partially esterified (60 mol %) using alkanoyl chlorides. The number of modified hydroxyl groups was controlled by the feed ratio. In the present case, fatty acid derivatives of varying chain length, namely lauric (C12), myristic (C14), and stearic (C18) acids, were employed. These derivatives were purposely chosen in order to study the influence of alkyl chain length on the properties of the reverse polymeric micelles.

The resulting  $\text{PG}_{\text{OH}}\text{MA-CX}$  derivatives (Figure 1) were water-insoluble but easily dissolved in organic solvents such as DCM and THF. Furthermore, all polymers were soluble in ethyl oleate, an oil approved for pharmaceutical use. Oleaginous polymeric solutions were prepared by dissolving the polymer in ethyl oleate at high temperature ( $60\text{ }^{\circ}\text{C}$ ) and then allowing the mixture to cool to room temperature. All star-shaped alkylated  $\text{PG}_{\text{OH}}\text{MA}$ s formed thermoreversible ethyl oleate organogels. Gel formation was observed at high concentration ( $>100\text{ g}\cdot\text{L}^{-1}$ ) for both the lauric and myristic acid derivatives, while  $\text{PG}_{\text{OH}}\text{MA-C18}$  induced gelation at a much lower concentration ( $\geq 10\text{ g}\cdot\text{L}^{-1}$ ). In all cases, the sol-gel transition occurred upon cooling and was attributed to a decrease of the affinity of the polymer for the dispersing phase.<sup>21</sup> Organogelation remains an intricate and often unpredictable process in which a combination of intermolecular attractive interactions, such as hydrogen bond forma-

(19) Kim, C.; Kim, K. T.; Chang, Y. *J. Am. Chem. Soc.* **2001**, *123*, 5586–5587.

(20) Garamus, V. M.; Maksimova, T.; Kautz, H.; Barriau, E.; Frey, H.; Schlotterbeck, U.; Mecking, S.; Richtering, W. *Macromolecules* **2004**, *37*, 8394–8399.

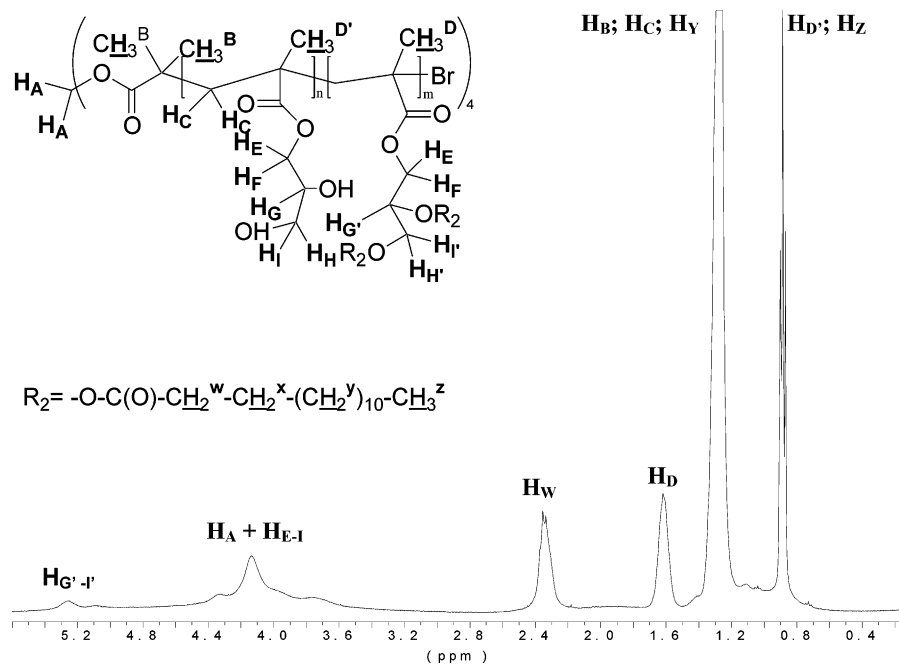
(21) Murdan, S.; Gregoriadis, G.; Florence, A. T. *J. Pharm. Sci.* **1999**, *88*, 608–614.



**Table 1.** Characterization of Alkylated PG<sub>OH</sub>MA<sub>S</sub>

polymer	PGMA properties				fatty acid derivatives			mean diameter (nm) [polydispersity index]	
	theor $M_n$	exptl $M_n$		$M_w/M_n$	chain length	DA (%)		ethyl oleate	THF
		by <sup>1</sup> H NMR <sup>a</sup>	by SEC			theor	exptl		
PG <sub>OH</sub> MA-C12	15 000	16 900	20 600	1.17	lauric (–OC(O)–(CH <sub>2</sub> ) <sub>10</sub> –CH <sub>3</sub> )	60	65.3	19 [0.3]	33 [0.24]
PG <sub>OH</sub> MA-C14					myristic (–OC(O)–(CH <sub>2</sub> ) <sub>12</sub> –CH <sub>3</sub> )	60	60.1	19 [0.3]	32 [0.25]
PG <sub>OH</sub> MA-C18					stearic (–OC(O)–(CH <sub>2</sub> ) <sub>16</sub> –CH <sub>3</sub> )	60	61.0	19 [0.3]	32 [0.24]

<sup>a</sup>  $M_n$  was calculated from the spectrum of PGMA using the intensities of the peaks at  $\delta = 3.22$  and 4.2 ppm (8H).

**Figure 1.** <sup>1</sup>H NMR spectrum of PG<sub>OH</sub>MA-C14 in CDCl<sub>3</sub>.

tion and van der Waals forces, are thought to participate.<sup>19,22</sup> In the present case, free stearyl chloride failed to produce an organogel in ethyl oleate at a similar concentration (10 g·L<sup>-1</sup>), thus confirming the determining role of hydrogen bonding. It should be mentioned that in all further experiments involving PG<sub>OH</sub>MA-C18, polymer concentrations were adjusted to prevent gelation.

**3.2. Reverse Micelle Characterization.** Micelle size was evaluated in both ethyl oleate and THF (Table 1). In ethyl oleate, micellar aggregates presented mean diameters of approximately 19 nm with a relatively broad size distribution (Table 1). The observed size did not vary between the different alkylated polymers. In THF, the average diameters experienced a 1.7-fold increase for all formulations (Table 1). The heightened polarity ( $\epsilon = 7.6$  vs 3.2 for ethyl oleate) of this solvent is thought to contribute to the observed occurrence. Indeed, it is possible that the more polar surrounding provided by THF induced the swelling of the hydrophilic core and exposed some of the hydroxyl functionalities, thus promoting the aggregation of the polymer. When compared to the diameters reported for dendrimers or hyperbranched structures with similar MWs (2–10 nm),<sup>12,20</sup> the sizes observed for star-shaped micelles tend to indicate that multimolecular rather than unimolecular micelles are formed.<sup>23</sup> Furthermore, the diameters observed by DLS in both solvents are higher than the theoretical diameter of a fully

extended star-shaped PG<sub>OH</sub>MA-CX (ca. 9–10 nm), which further supports the hypothesis that alkylated PG<sub>OH</sub>MA<sub>S</sub> assemble into supramolecular structures in apolar media.

The morphology of the self-assembled nanocages in oil and THF was elucidated by AFM and cryo-TEM, respectively (Figure 2). In both solvents, spherical aggregates were observed, and the average diameters and polydispersity correlated well with the light scattering results (see Supporting Information). To date, cryo-TEM has been applied mainly to imaging in aqueous environments,<sup>24,25</sup> low-viscosity organic solvents,<sup>26,27</sup> or ionic liquids;<sup>28</sup> its utilization for oleaginous media is restricted due to inherent difficulties in sample preparation.<sup>29</sup> However, the results presented here (Figure 2b) confirm the feasibility of using cryo-TEM to study the self-assembly of polymeric amphiphiles in oils.

### 3.3. Protein Partition between Ethyl Oleate and Water.

#### 3.3.1. Extraction of Vasopressin.

The ability of PG<sub>OH</sub>MA-

(22) Motulsky, A.; Lafleur, M.; Couffin-Hoarau, A. C.; Hoarau, D.; Boury, F.; Benoit, J. P.; Leroux, J. C. *Biomaterials* **2005**, *26*, 6242–6253.

(23) Krämer, M.; Stumbé, J.-F.; Türk, H.; Krause, S.; Komp, A.; Delineau, L.; Prokhorova, S.; Kautz, H.; Haag, R. *Angew. Chem., Int. Ed.* **2002**, *41*, 4252–4256.  
 (24) Pochan, D. J.; Chen, Z. Y.; Cui, H. G.; Hales, K.; Qi, K.; Wooley, K. L. *Science* **2004**, *306*, 94–97.  
 (25) Wittemann, A.; Drechsler, M.; Talmon, Y.; Ballauff, M. *J. Am. Chem. Soc.* **2005**, *127*, 9688–9689.  
 (26) Balmes, O.; Malm, J.-O.; Karlsson, G.; Bovin, J.-O. *J. Nanopart. Res.* **2004**, *6*, 569–576.  
 (27) Boettcher, C.; Schade, B.; Fuhrhop, J.-H. *Langmuir* **2001**, *17*, 873–877.  
 (28) He, Y. Y.; Li, Z. B.; Simone, P.; Lodge, T. P. *J. Am. Chem. Soc.* **2006**, *128*, 2745–2750.  
 (29) Danino, D.; Gupta, R.; Satyavolu, J.; Talmon, Y. *J. Colloid Interface Sci.* **2002**, *249*, 180–186.

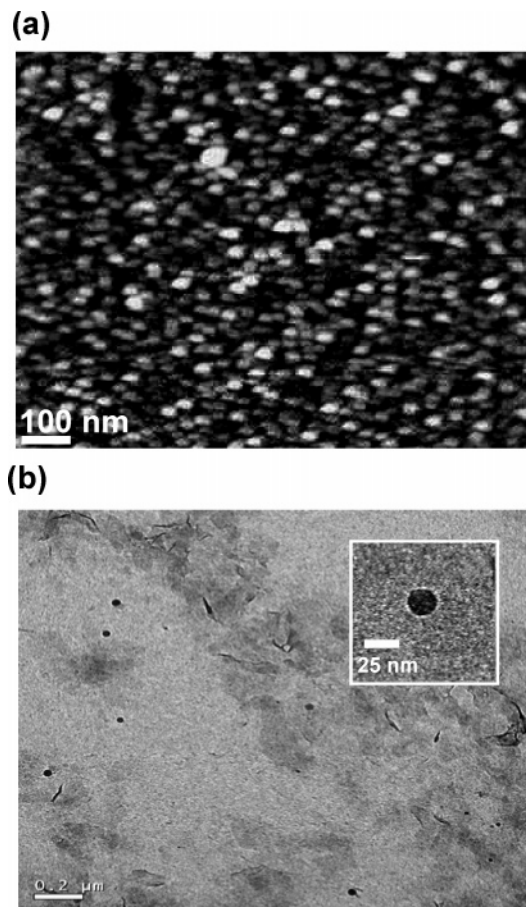


**Figure 2.** Study of the morphology of reverse  $\text{PG}_{\text{OH}}\text{MA-C18}$  micelles. The morphology of  $\text{PG}_{\text{OH}}\text{MA-C18}$  was studied by (a) AFM in THF and (b) cryo-TEM in ethyl oleate. The inset shows a magnified RPM.

CX RPMs to take up a water-soluble macromolecule in ethyl oleate was first demonstrated through partition studies using vasopressin, a natural peptide (1084 Da) which plays an important role in the regulation of extracellular fluid levels in the human organism. The encapsulation of vasopressin was studied as a function of peptide concentration (0.25–10 wt % of polymer). RPMs were loaded with vasopressin by mixing solutions of the polymer in DCM/ethyl oleate with ethanolic solutions of the peptide. The volatile organic solvents were then removed to allow the incorporation of vasopressin. Particle size analysis performed at that point revealed a 3- to 4-fold increase in micelle size, with  $\text{PG}_{\text{OH}}\text{MA-C18}$  experiencing the most change with diameters around 65–70 nm. The aqueous phase was then added in order to extract the un-incorporated peptide. In the absence of micelles, vasopressin was only marginally retained in the oleaginous phase (<5%;  $K_{\text{app}} < 0.05$ ) and partitioned preferentially into the aqueous layer. Linear  $\text{PG}_{\text{OH}}\text{MA-CX}$  also failed to take up considerable amounts of vasopressin in ethyl oleate (data not shown), emphasizing the importance of the polymer structure.<sup>30,31</sup> The addition of RPMs, however, led to a significant increase in the quantity of peptide solubilized in the organic phase. As vasopressin exhibited limited affinity for the oleaginous phase, its partition in the organic phase is attributed to its loading in the micellar core.

(30) Stiriba, S.-E.; Kautz, H.; Frey, H. *J. Am. Chem. Soc.* **2002**, *124*, 9698–9699.

(31) Chen, Y.; Shen, Z.; Pastor-Pérez, L.; Frey, H.; Stiriba, S.-E. *Macromolecules* **2005**, *38*, 227–229.

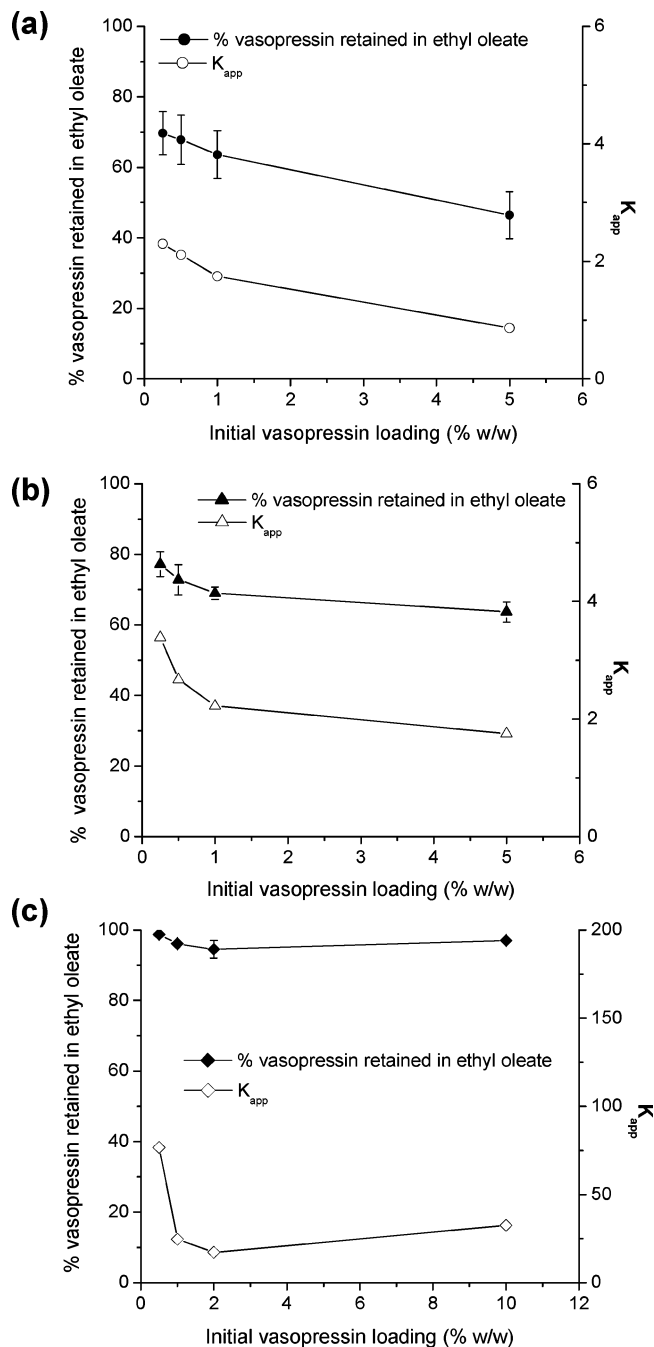


**Figure 3.** Partition of vasopressin between ethyl oleate and water in the presence of RPMs of (a)  $\text{PG}_{\text{OH}}\text{MA-C12}$ , (b)  $\text{PG}_{\text{OH}}\text{MA-C14}$ , and (c)  $\text{PG}_{\text{OH}}\text{MA-C18}$ . The results for the amount (%) of vasopressin retained (closed symbols) are presented as the mean  $\pm$  SEM of at least three independent experiments. The partition coefficient ( $K_{\text{app}}$ ; open symbols) was estimated using eq 3. The initial loadings are expressed in wt % of polymer (2.5 or 5 mg).

The retention efficiency of vasopressin in the RPMs was influenced by both the nature of the star-shaped polymer and the initial peptide loading (Figure 3). Under the tested experimental conditions,  $\text{PG}_{\text{OH}}\text{MA-C12}$  reverse micelles were able to retain 0.2–2.4% of their weight of vasopressin in the oil phase, corresponding to entrapment efficiencies between  $46.4 \pm 6.6\%$  and  $69.7 \pm 6.2\%$  and  $K_{\text{app}}$  values between 0.9 and 2.3 (Figure 3a).  $\text{PG}_{\text{OH}}\text{MA-C14}$  showed higher retention efficacy, with partition coefficients between 1.8 and 3.4 (Figure 3b). The stearic acid derivative was the most effective, with up to 10%

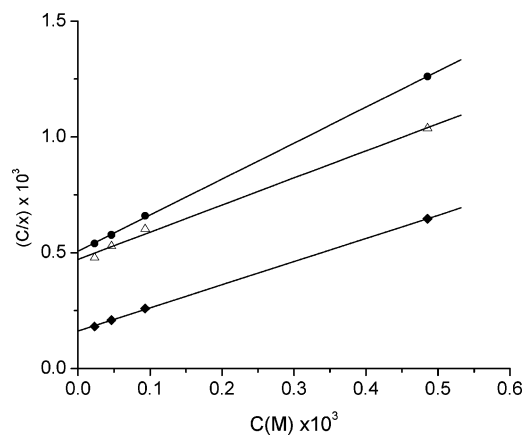


**Figure 4.** Fitting of the partition data according to the Langmuir isotherm for PG<sub>OH</sub>MA-C12 (closed circles), PG<sub>OH</sub>MA-C14 (open triangles), and PG<sub>OH</sub>MA-C18 (closed diamonds).

of its weight in vasopressin solubilized in ethyl oleate and efficiencies ranging from  $94.5 \pm 2.5\%$  to  $98.7 \pm 0.7\%$ . Accordingly, in the presence of PG<sub>OH</sub>MA-C18 micelles, the peptide concentrations were 17–77 times higher in oil than in water (Figure 3c). The remarkable ability of this formulation to retain vasopressin in ethyl oleate may be attributed to the higher lipophilicity of the C18 shell. The C18 chains may act as a barrier that prevents the entrapped peptide from migrating into the apolar external phase, where it could be extracted by water molecules.<sup>15,23</sup>

In all cases, the  $K_{app}$  values were inversely related to guest concentration. Peptide molecules that are taken up by the reverse micelles may slowly fill the core–shell interface until the space is completely occupied; from this point forward, excess peptide is transferred to the aqueous phase, shifting the  $K_{app}$  toward lower values.<sup>13</sup> The Langmuir adsorption isotherm was thus applied to evaluate the maximum amount of peptide that can be accommodated<sup>32</sup> (Figure 4).

The Langmuir isotherm is based on the premise that solutes will adsorb onto a surface to form a monomolecular layer and is described by eq 4,

$$\frac{C}{x} = \frac{1}{x_{max}K_{ads}} + \frac{C}{x_{max}} \quad (4)$$

where  $C$  is the molar concentration of peptide,  $x$  is the mole fraction of peptide in the micellar phase,  $x_{max}$  is the maximum of that mole fraction value, and  $K_{ads}$  is the Langmuir adsorption constant.

The partition data fitted well with the Langmuir model ( $r^2 > 0.99$ ), supporting the hypothesis that loading can reach saturation and occurs at the core–shell interface.<sup>32,33</sup> Interestingly, the value of the slope was influenced by the nature of the hydrophobic segment (Figure 4). The slope was more pronounced for the C12 and C14 derivatives compared to PG<sub>OH</sub>MA-C18, yielding  $x_{max}$  values of 0.64, 0.85, and 0.99, respectively (Table 2). These experimental  $x_{max}$  values were used to compute the maximum amount of drug that can be accommodated within the RPMs (Table 2). As expected, PG<sub>OH</sub>MA-C18 showed the highest solubilization capacity of all formulations, which corroborates the partition data.

**Table 2.** Maximum Protein Loading in RPMs

RPM	vasopressin (MW 1048)		myoglobin (MW 17 600)		FITC-albumin (MW 66 000)	
	$x_{max}$	DL <sub>max</sub> <sup>a</sup> (% w/w)	$x_{max}$	DL <sub>max</sub> <sup>a</sup> (% w/w)	$x_{max}$	DL <sub>max</sub> <sup>a</sup> (% w/w)
PG <sub>OH</sub> MA-C12	0.64	6.5	0.08	5.0	n.d.	n.d.
PG <sub>OH</sub> MA-C14	0.85	17.8	0.07	4.2	n.d.	n.d.
PG <sub>OH</sub> MA-C18	0.99	77.0	0.07	3.8	0.009	1.7

<sup>a</sup> Maximum drug loading. “n.d.” indicates not determined.

**3.3.2. Extraction of Myoglobin and Albumin.** The results obtained with vasopressin demonstrate that RPMs are able to interact with a hydrophilic molecule and to significantly increase its solubility in an oleaginous phase. The RPM’s extraction capability was further challenged using a more complex polypeptide, namely myoglobin. Myoglobin is a 17 600 Da protein responsible for the transport and storage of oxygen in the muscles. Unlike vasopressin, myoglobin presents an elaborate tri-dimensional structure, which could be destroyed in the presence of ethanol. As a result, the loading method was adapted to avoid the use of potentially deleterious solvents.

As expected, increasing the MW of the guest molecule resulted in decreases of the loading efficiency and the  $K_{app}$  value (see Supporting Information). Still, the reverse micelles were able to load approximately 1.3–2.9% of their weight in myoglobin, with PG<sub>OH</sub>MA-C18 showing the best results. At low concentrations (1–2 wt%), the latter extracted over 80% of the myoglobin present in the aqueous phase, while PG<sub>OH</sub>MA-C12 and PG<sub>OH</sub>MA-C14 took up approximately 50% of the protein. The slight difference in efficacy previously observed between the two shorter-chained RPMs disappeared with the increase in guest size. The C12 derivative even proved to be somewhat more efficient in extracting myoglobin than PG<sub>OH</sub>MA-C14.

The  $K_{app}$  values remained above unity at the lowest initial loading tested, confirming that RPMs were able to improve the partition of myoglobin between oil and water. For all formulations, the  $K_{app}$  values decreased steadily over the range of concentrations studied (see Supporting Information).

The myoglobin partition data were fitted using the Langmuir isotherm (eq 4). Contrary to what was observed with vasopressin, there was no difference between the slopes of the different RPM formulations. Replacing vasopressin by myoglobin led to an 8- to 13-fold decrease in the  $x_{max}$  value (Table 2), which correlates well with the fact that this protein is 16 times larger than vasopressin. The maximum loading values for myoglobin are reported in Table 2. The loading was highest for PG<sub>OH</sub>MA-C12 (5% w/w) and decreased slightly with lengthening of the hydrophobic chain, in opposition to what was seen for vasopressin. This difference may be ascribed to both the MW of the encapsulated compounds and the extraction methods. Vasopressin was first loaded inside the micelles with the help of ethanol and then extracted back with the aqueous phase. To avoid using an organic solvent in the presence of a protein, myoglobin was first dissolved in the aqueous buffer and then incubated with the oleaginous RPM solution. As a consequence, augmenting the length of the hydrocarbon chain may increase steric hindrance and thus lower the drug loading. Moreover, since myoglobin forms aggregates of 3–4 nm in aqueous solutions (one-sixth of the micellar size), its diffusion through a highly shielded micelle core may be impaired.

(32) Choucair, A.; Eisenberg, A. *J. Am. Chem. Soc.* **2003**, *125*, 11993–12000.

(33) Croy, S. R.; Kwon, G. S. *J. Pharm. Sci.* **2005**, *94*, 2345–2354.

To further investigate the effect of MW on uptake, a 66 000 Da serum protein (i.e., albumin) was selected for encapsulation into PG<sub>OH</sub>MA-C18 RPMs. Albumin is known to interact with hydrophobic compounds, such as lauric and myristic acids. However, it has been shown that conformational rigidity limits its interactions with neutral fatty acids containing over 14 carbon atoms;<sup>34,35</sup> the nonspecific adsorption of PG<sub>OH</sub>MA-C18 RPMs and oil adsorption should therefore remain negligible. The extraction ability of the PG<sub>OH</sub>MA-C18 RPMs was influenced by the initial protein concentration, similar to what was observed for vasopressin and myoglobin. Although significantly lower than those observed for vasopressin or myoglobin, the maximal partition coefficient remained above unity at initial concentrations below 2% (see Supporting Information). Albumin partitioned preferentially in water at concentrations above this threshold. Fitting the partition data to the Langmuir isotherm yielded an  $x_{\max}$  value of  $9.0 \times 10^{-3}$ , which corresponds to a 116- and 8.5-fold decrease compared to the values obtained for vasopressin and myoglobin, respectively (Table 2). Further proof of the more favorable interaction of PG<sub>OH</sub>MA-C18 RPM with smaller proteins was provided through a kinetic study of the loading. In the case of vasopressin, where the peptide is loaded in the RPM prior to extraction with water, the time dependency of guest loading was not evaluated. For both myoglobin and albumin, maximum loading was achieved in approximately 1 h. After 30 min, RPMs had extracted ~20% of albumin from the aqueous phase, compared to ~40% for myoglobin. Although PG<sub>OH</sub>MA-C18 micelles remain somewhat effective in promoting

the solubilization of albumin, albeit at lower concentration than vasopressin or myoglobin, the analysis of the partition data indicates that these micelles are better suited for the encapsulation of poly(amino acid)s with a MW between those of vasopressin and myoglobin.

#### 4. Conclusion

Hydrophobically modified star-shaped PG<sub>OH</sub>MA were successfully employed as building blocks for supramolecular assemblies in a pharmaceutically acceptable oil. These RPMs were able to drastically increase the solubility of various proteins including vasopressin, myoglobin, and, to a lesser extent, albumin in ethyl oleate. The nature of the hydrophobic segment and the guest molecule had a marked influence on the solubilizing ability of the reverse micelles. After additional processing, the system described here could be applied to the oral delivery of fragile peptidic molecules<sup>11</sup> or for their sustained release following parenteral extravascular injection.<sup>36</sup>

**Acknowledgment.** This work was financially supported by the Natural Sciences and Engineering Research Council of Canada and Mistral Pharma Inc. (Montreal, QC, Canada). M.C.J. acknowledges a scholarship from the Fonds de la Recherche en Santé du Québec. Financial contribution from the Canada Research Chair program and NSF NIRT (Grant No. DMR-0210247) is also recognized.

**Supporting Information Available:** AFM picture of four-arm star-shaped PG<sub>OH</sub>MA, extraction of myoglobin by RPMs, and extraction of albumin by RPMs. This material is available free of charge via the Internet at <http://pubs.acs.org>.

JA065462C

- (34) Bird, D. A.; Laposata, M.; Hamilton, J. A. *J. Lipid Res.* **1996**, *37*, 1449–1458.  
(35) Ashbrook, J. D.; Spector, A. A.; Santos, E. C.; Fletcher, J. E. *J. Biol. Chem.* **1975**, *250*, 2333–2338.

- (36) Plourde, F.; Motulsky, A.; Couffin-Hoarau, A. C.; Hoarau, D.; Ong, H.; Leroux, J. C. *J. Controlled Release* **2005**, *108*, 433–441.